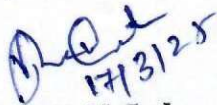


## CERTIFICATE

It is certified that the work contained in the thesis titled "*Electrolytic Capacitor-Less Resonant Power Converters for Solar PV Applications*" by "*Prakash Ji Barnawal*" has been carried out under my supervision and this work has not been submitted elsewhere for a degree.

It is further certified that the student has fulfilled all the requirements of Comprehensive, Candidacy and SOTA for the award of Ph.D. Degree.

**Supervisor**



**Prof. V. N. Lal**

Associate Professor

Department of Electrical Engineering

Indian Institute of Technology (BHU)

Varanasi-221005

**Co-Supervisor**



**Prof. R. K. Singh**

Professor

Department of Electrical Engineering

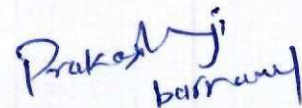
Indian Institute of Technology (BHU)

Varanasi-221005

## DECLARATION BY THE CANDIDATE

I, **Prakash Ji Barnawal**, certify that the work embodied in this thesis is my own bonafide work and carried out by me under the supervision of **Prof. V. N. Lal and Prof. R. K. Singh** from **July 2019 to March 2025** at the **Department of Electrical Engineering**, Indian Institute of Technology (Banaras Hindu University), Varanasi. The matter embodied in this thesis has not been submitted for the award of any other degree/diploma. I declare that I have faithfully acknowledged and given credits to the research workers wherever their works have been cited in my work in this thesis. I further declare that I have not wilfully copied any other's work, paragraphs, text, data, results, *etc.*, reported in journals, books, magazines, reports dissertations, thesis, *etc.*, or available at websites and have not included them in this thesis and have not cited as my own work.

Date: **17/03/2025**  
Place: Varanasi



Signature of the Student  
(Prakash Ji Barnawal)

## CERTIFICATE BY THE SUPERVISOR

It is certified that the above statement made by the student is correct to the best of my knowledge.



Supervisor  
(Prof. V. N. Lal)



Co-Supervisor

(Prof. R. K. Singh)

  
17/3/25

Head of Department

Department of Electrical Engineering

विद्युतीय अभियंत्रिकी विभाग / Department of Electrical Engineering  
भारतीय प्रौद्योगिकी संस्थान / Indian Institute of Technology  
वाराणसी हिन्दू विश्वविद्यालय / (Banaras Hindu University)  
Varanasi (U.P.) (INDIA)

## COPYRIGHT TRANSFER CERTIFICATE

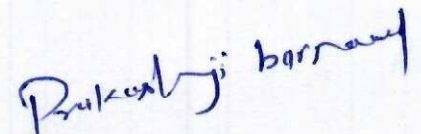
**Title of the Thesis:** Electrolytic Capacitor-Less Resonant Power Converters for Solar PV Applications

**Name of the Student:** Prakash Ji Barnawal

### Copyright Transfer

The undersigned hereby assigns to the Indian Institute of Technology (Banaras Hindu University) Varanasi all rights under copyright that may exist in and for the above thesis submitted for the award of the "*Doctor of Philosophy*".

Date: 17/3/2025  
Place: Varanasi



Signature of the Student  
(Prakash Ji Barnawal)

**Note:** However, the author may reproduce or authorize others to reproduce material extracted verbatim from the thesis or derivative of the thesis for the author's personal use, provided that the source and the Institute's copyright notice are indicated.

*Dedicated*  
*to*  
*My Family and VLPERI*

# Content

<b>Abstract</b>	vii
<b>Acknowledgment</b>	xi
<b>List of Figures</b>	xiii
<b>List of Tables</b>	xvii
<b>List of Acronyms</b>	xix
<b>Symbols Used</b>	xxi
<b>Chapter 1. Introduction</b> .....	1
<b>1.1</b> Background and Motivation.....	1
<b>1.2</b> Literature Survey on Isolated DC-DC Converters .....	4
<b>1.2.1</b> Voltage-fed Isolated DC-DC Converters (PWM-type) .....	4
<b>1.2.2</b> Current-fed Isolated DC-DC Converters (PWM-type): .....	7
<b>1.2.3</b> Isolated DC-DC Converters (Resonant-type).....	9
<b>1.2.4</b> Impedance Network-based Isolated Converters .....	10
<b>1.2.5</b> Vulnerability of the Electrolytic Capacitors in Power Converters .....	12
<b>1.2.6</b> Maximum Power Point Tracking under Partial Shading Conditions .....	13
<b>1.3</b> Challenges with the Existing Systems .....	15
<b>1.4</b> Objective of the Thesis.....	16
<b>1.5</b> Organization of the Thesis .....	18
<b>Chapter 2. Electrolytic Capacitor-less Isolated DC-DC Resonant Converters</b> .....	21
<b>2.1</b> Introduction.....	21
<b>2.2</b> Proposed Converter -1 (Dual-Half Active Bridge Resonant Converter) .....	21
<b>2.3</b> Operation of the Proposed DHABRC .....	22

2.3.1 Interval 1: ( $T_0 - T_1$ ) Fig. 2.3 (a) .....	23
2.3.2 Interval 2: ( $T_1 - T_2$ ) Fig. 2.3 (b) .....	23
2.3.3 Interval 3: ( $T_2 - T_3$ ) Fig. 2.3 (c) .....	25
2.3.4 Interval 4: ( $T_3 - T_4$ ) Fig. 2.3 (d) .....	25
2.3.5 Interval 5: ( $T_4 - T_5$ ) Fig. 2.3 (e) .....	26
2.3.6 Interval 6: ( $T_5 - T_6$ ) Fig. 2.3 (f) .....	26
2.3.7 Interval 7: ( $T_6 - T_7$ ) Fig. 2.3 (g) .....	26
2.3.8 Interval 8: ( $T_7 - T_8$ ) Fig. 2.3 (h) .....	26
2.4 Proposed Converter -2 (Asymmetrical Dual Active Bridge Resonant Converter) .....	26
2.5 Operation of the Proposed ADABRC .....	28
2.6 Steady-State Analysis of Proposed Resonant Converters Using FHA .....	28
2.6.1 Mathematical Model .....	28
2.6.2 Bridge Currents and Voltages .....	29
2.6.3 Equivalent AC Impedance .....	31
2.6.4 Gain of the Converter .....	31
2.6.5 Necessary Condition for ZVS .....	32
2.6.6 Sufficient Condition for ZVS and Effect of Dead Time .....	33
2.7 Design Optimization for the Proposed Converter DHABRC .....	35
2.7.1 Selection of Normalized Switching Frequency (F) .....	35
2.7.2 Selection of the Quality Factor (Q) .....	35
2.7.3 Selection of Converter Gain (M) .....	36
2.7.4 Inductance Ratio (K), Tank Components, and Dead Time .....	37
2.7.5 Voltage Stress .....	38
2.7.6 Design of the Film Capacitors .....	38
2.8 Results for DHABRC .....	40
2.8.1 Simulation Results .....	40
2.8.2 Experimental Results .....	42

2.8.3	Verification of the Efficacy of Analysis .....	44
2.8.4	Verification of using Film Capacitor .....	44
2.9	Results for ADABRC .....	47
2.9.1	Simulation Results .....	47
2.9.2	Experimental Results .....	50
2.10	Efficiency Analysis .....	51
2.11	Comparison with Similar Topologies .....	51
2.12	Conclusion .....	52
<b>Chapter 3. Solar PV Integration of Electrolytic Capacitor-less Isolated DC-DC Resonant Converter .....</b>		<b>53</b>
3.1	Introduction .....	53
3.2	Solar PV Integration of Dual Half Active Bridge Resonant Converter .....	53
3.3	Particle Swarm Optimization .....	54
3.4	Simulation Results for PSCs using PSO .....	58
3.5	Experimental Results for PSCs using PSO .....	62
3.6	Grey Wolf Optimization (GWO) .....	65
3.7	Experimental Results under GWO .....	68
3.7.1	Results under Uniform Irradiance Conditions (UIC) .....	68
3.7.2	Results under Partial Shading Conditions (PSCs) .....	69
3.8	Comparison with the Existing Converters .....	73
3.9	Conclusion .....	74
<b>Chapter 4. Pseudo DC-Link Based Two-Stage Topology for Solar PV to Grid-Tied System .....</b>		<b>75</b>
4.1	Introduction .....	75
4.2	Design of the Phase Locked Loop (PLL) .....	76

4.2.1 Transformation of Reference Frames/ Coordinate Systems .....	76
4.2.2 Design of the PLL control using PI controller .....	80
4.2.3 Design of the PLL control using K-factor Controller.....	81
4.2.4 Simulation Results Corresponding the PI and the K-factor Controller .....	83
4.3 State-space Modelling of the Voltage Source Inverter (VSI) .....	84
4.4 Design of the Inner Current Control Loop.....	86
4.4.1 Plant Transfer Function for the Current Control .....	86
4.4.2 PI Controller for Current Control .....	87
4.4.3 Complete Open Loop Transfer function.....	88
4.4.4 Modulus Optimum Tuning Criterion.....	89
4.5 Design of the Outer Voltage Control Loop.....	91
4.5.1 Plant Transfer Function for the Voltage Control.....	92
4.5.2 PI Controller for Voltage Control.....	93
4.5.3 Equivalent Inner Current Control Loop.....	93
4.5.4 Revised Open Loop Transfer function .....	94
4.5.5 Symmetrical Optimum Tuning Criterion (SOTC).....	95
4.6 Design of the LC Filter .....	97
4.7 Pseudo DC Link Capacitor Required.....	97
4.8 Simulation Results Under PSCs With Resistive Load.....	99
4.9 Experimental Results Under PSCs with Resistive Load.....	102
4.10 Simulation Results for Solar PV to Grid-Tied Condition.....	105
4.11 Conclusion .....	107

**Chapter 5. Expandable Input Impedance-Sourced Isolated DC-DC Resonant Converter**  
..... 109

5.1 Introduction.....	109
5.2 Proposed converter.....	110

<b>5.3</b>	Expandable input impedance-sourced network (EIIS) .....	110
<b>5.3.1</b>	DTs Switching State .....	110
<b>5.3.2</b>	(1-D) $T_s$ Switching State.....	112
<b>5.4</b>	Expandable Input Impedance Sourced Isolated Resonant Converter .....	116
<b>5.4.1</b>	Interval I: ( $T_0 - T_1$ ) .....	116
<b>5.4.2</b>	Interval II: ( $T_1 - T_2$ ).....	116
<b>5.4.3</b>	Interval III: ( $T_2 - T_3$ ) .....	116
<b>5.5</b>	PSO Algorithm for PSC .....	118
<b>5.6</b>	Design of the Converter .....	119
<b>5.6.1</b>	Modeling of the IRC.....	120
<b>5.6.2</b>	Calculation of Voltage Gain and Power .....	121
<b>5.6.3</b>	Soft-Switching Realization.....	121
<b>5.7</b>	Design of the Proposed Topology.....	122
<b>5.7.1</b>	Normalized Switching Frequency (F) .....	122
<b>5.7.2</b>	Gain ( $\lambda$ ), turns ratio ( $n_i$ ), and Inductance Ratio ( $K$ ).....	122
<b>5.7.3</b>	Quality Factor .....	123
<b>5.7.4</b>	Resonant Components .....	124
<b>5.7.5</b>	Design of the EIIS Network Inductors .....	124
<b>5.7.6</b>	Design of Film Capacitors of the EIIS Network .....	124
<b>5.7.7</b>	Design of Film Capacitors (FC) of IRC .....	125
<b>5.8</b>	Experimental Verification.....	127
<b>5.8.1</b>	Steady State Results for Proposed Expandable Input Impedance Sourced Isolated Resonant Converter .....	127
<b>5.8.2</b>	Experimental Results for Soft-switching.....	130
<b>5.8.3</b>	Results Under Uniform Irradiance Conditions .....	132
<b>5.8.4</b>	Results Under PSCs and Dynamic Irradiance Conditions.....	132
<b>5.8.5</b>	Verification of Film Capacitor Usage .....	135

5.9 Design Flexibility with EHS and Inegration with Grid System.....	136
5.10 Conclusion.....	138
<b>Chapter 6. Conclusion and Scope of Future Work.....</b>	<b>139</b>
6.1 Introduction.....	139
6.2 Conclusion .....	139
6.3 Scope of the Future Work .....	141
<b>Bibliography.....</b>	<b>143</b>
<b>List of Publications .....</b>	<b>163</b>

# Abstract

Renewable energy sources, particularly solar photovoltaic (PV) systems, have emerged as a prominent solution to address the current power crisis and pressing environmental concerns. In recent years, there has been a substantial increase in the installation capacity of solar PV systems worldwide. However, the power generated from solar PV systems is non-linear and depends on unpredictable environmental and shading conditions. So, a reliable and efficient power converter integrated with maximum power point tracking (MPPT) control is needed to harness and utilize solar power effectively. Photovoltaic (PV) systems employ silicon-based cells to convert solar energy into electrical energy. When the solar irradiance falling on the solar panel is uniform, a power-voltage curve (PV curve) with a single peak is observed. In contrast, a multi-peak PV curve is observed when there is any obstruction in the path of sunlight or when panels are shaded. Using conventional maximum power point tracking (MPPT) algorithms like perturb and observe (P&O) and incremental conductance (INC), maximum power can be harnessed. However, the conventional algorithm faces difficulty under a multi-peak PV curve and fails to harness the power at the global maxima point. A heuristic algorithm is required to harness maximum under multi-peak PV curves. Since solar power is of a DC nature, a DC-DC or DC-AC power converter can be employed for the power interface. The isolated class DC-DC converter can be preferred over the non-isolated one for DC-DC converters when high voltage application, safety, and compliance are top priorities. The galvanic isolation of the isolated DC-DC converter ensures safe and leakage-free operation for two-stage DC-AC topologies. The high-frequency operation of the isolated DC-DC converter reduces the volume and size of the converter concurrently, increasing the switching losses of the converter. Some isolated DC-DC converters, like a dual active bridge, use their transformer leakage inductance to achieve zero voltage switching operation. However, they suffer from light load efficiencies. Resonant tanks can reduce switching losses by releasing the energy stored within the switching devices. A resonant tank can be employed in series, parallel, or series-parallel combinations. However, they pose various design complexities and constraints. These isolated resonant converters can be further categorized as load resonant converters and quasi-resonant converters based on utilizing the switching cycle. These isolated converters often use switching schemes with complementary gating signals that require a small dead-band time between them to avoid the short circuit between the power rails. The dead-band time needed for these converters can be optimized to enhance soft-switching while affecting the tank

elements. In power converters, electrolytic capacitors are often utilized as voltage-smoothing filters to stabilize the DC voltage despite their vulnerable and unreliable operation. These electrolytic capacitors suffer from the aging effect; as their electrolytes evaporate with time, their capacitance decreases, and equivalent series resistance increases with time. If these electrolytic capacitors are employed for voltage smoothing in solar PV converters, they may need to be replaced several times over a single solar panel life span. Besides this, continuous health monitoring is also required to track their physical degradation to avoid future consequences. The film capacitor can be a better alternative for low to medium-power applications as it doesn't age with time and has no physical limitations, making it more suitable for solar PV applications. Besides this, the rms current rating per unit capacitance of the film capacitor can be twenty to fifty times higher than that of the electrolytic capacitors. To address the vulnerability of the electrolytic capacitors, some electrolytic capacitor-less isolated two-stage topologies have been given. However, the voltage at the DC link is pulsating, requiring a novel modulation scheme to operate the inverter. Due to the pulsating voltage at the DC link, energy storage systems can't be integrated at the DC link. Also, these topologies have not been tested for solar PV integration.

To resolve the issue associated with the use of electrolytic capacitors, electrolytic capacitor-less isolated DC-DC converters, dual half-active bridge resonant converters (DHABRC) for low power application, and asymmetrical dual half-active bridge resonant converters (ADABRC) for low to medium-power applications have been proposed. The proposed converters utilize film capacitors for voltage smoothing for better reliability. The proposed converters have been analyzed and designed using the fundamental harmonics approximation. The sufficient and necessary conditions for soft-switching have been derived to optimize the dead band time required to operate the proposed converter. An optimized LLC resonant tank has improved the converter's efficiency. The film capacitor of the LLC tank blocks the DC current, preventing DC voltage imbalances, particularly those arising from output-side film capacitors, from saturating the high-frequency transformer. The efficacy of the FHA technique has been verified by comparing the theoretical data obtained from the analysis with simulation and experimental results. A hardware setup of 500W is developed and tested for steady-state and soft-switching conditions. From the experimental results, the zero-voltage switching operation of all the active switches has been verified. The feasibility of using film capacitors has also been verified by measuring the voltage under startup transient, load dynamics, and steady-state conditions.

The proposed converter is further integrated with solar PV. For this, a solar PV emulator ((Chroma 62100H-600S) has been used, and multiple PV curves of different power ratings are generated for uniform and non-uniform irradiance conditions (partial shading conditions). The simulation and experimental tests have been performed for the 500 W converter. The maximum power at the global maxima point has been drawn using particle swarm optimization and grey wolf optimization. The heuristic algorithm offers many advantages, such as tracking global peak power under PSC, adaptability to dynamic conditions, fewer oscillations, less sensitivity to noise, less mathematical complexities, and a direct control approach, causing the elimination of the control loops. The steady-state oscillations in voltage and current waveforms are also negligible around the steady-state conditions.

Next, the proposed converter is connected to a three-phase voltage source inverter (VSI) to feed the power to the resistive load and AC grid, forming a pseudo-DC link-based isolated two topology. In the two-stage topology, the need for the DC link capacitor is eliminated, and the outer film capacitor leg of the isolated DC-DC converter is utilized to act like a DC link. The inverter output is synchronized to the grid's characteristics using a synchronous reference frame-based phase-locked loop. The control loop designed for the topology ensures the quality of the grid current with over-current protection. The voltage control loop provides the stable DC link voltage while balancing the power flow at the DC link. The PI controller of the inner current control loop is tuned using the modulus optimum tuning criterion. The PI controller of the outer voltage control loop is tuned using the symmetrical optimum tuning criterion. The proposed two-stage is first tested for resistive load and then tested to feed the power to the three-phase AC grid. The proposed pseudo-DC link-based two-stage topology easily transfers the solar power to the AC grid.

The low voltage output generated from solar PV needs to be stepped up to the utility/microgrid voltage level for efficient utilization. An impedance network is added at the input side of the electrolytic capacitor-less isolated DC-DC converters. The impedance network accommodates a wide range of input PV voltage while ensuring a regulated DC output. This is achieved by dynamically adjusting the duty cycle. Furthermore, the impedance network enhances system resilience by mitigating the risk of shoot-through faults and short circuits that may occur due to misfiring events, thereby improving the system's immunity to electromagnetic interference (EMI). The utilized impedance network exhibits an expandable architecture. With each additional stage added to the network, the overall voltage gain of the system increases. Thus, an expandable input impedance-sourced isolated resonant converter

(EISIRC) with electrolytic capacitor-less properties is formed. For the proposed EISIRC, a hardware prototype of 500 W is built, which is later tested for steady-state and partial-shaded conditions.

# Acknowledgment

Undertaking this PhD has been a profoundly transformative experience for me, and it would not have been possible without the support and guidance I received from many people. First, I owe **Lord Shiva** for calling me to the ancient city of Varanasi, granting me the wisdom, health, and strength to undertake this research task, and enabling me to complete it.

Foremost, I would like to express my sincere gratitude to my supervisors, **Dr. Vivek Nandan Lal** and **Prof. Rajeev Kumar Singh**, for giving me the opportunity to work on this interesting research work. Their insightful guidance, constant encouragement, and unwavering belief in my abilities have inspired me to complete this research successfully. I am indebted to both supervisors for giving me abundant freedom to pursue new ideas. It was an excellent opportunity to do my doctoral program under their guidance and learn from their research expertise. Their guidance helped me immensely in all the research work and thesis writing. I could not have imagined having such better mentors for my PhD study.

Besides my supervisors, I would like to thank the members of my research progress evaluation committee: **Prof. Ranjit Mahanty**, Professor, Department of Electrical Engineering, **Prof. Sanjay Kumar Singh**, Professor, Department of Computer Science & Engineering, for their encouragement, insightful comments, and suggestions in various presentations during my research work tenure. I am grateful to the reviewers whose constructive suggestions and invaluable advice improved the quality of my publications derived from this work.

I want to acknowledge again **Prof. Rajeev Kumar Singh**, Head of the Department of Electrical Engineering, for his help on various occasions. Moreover, I am highly obliged to sincerely thank the technical, non-technical, and administrative staff of the Electrical Engineering department, who helped me in all possible ways during the work.

I want to express my sincere gratitude to the professors for their collective efforts in establishing the **VLPERI** research group (**Virtuous Lab of Power Electronics Research & Innovation**). Their dedication has created an exceptional research environment and infrastructure for all scholars. I am deeply grateful to have been a part of **VLPERI** since its start. I appreciate their commitment to fostering a conducive workspace, a stimulating atmosphere, and a vibrant research ecosystem. I consider it a privilege to have had the opportunity to learn from their expertise. Thank you, Professors, for your guidance and support.

I would like to express my sincere gratitude to my senior colleagues, Dr. Pawan Kumar, Dr. Soumya Ranjan Meher, Dr. Manash Kumar Mishra, and Dr. Simanta Kumar Samal, for their invaluable guidance and support during the formative stages of my research. I am also profoundly grateful to my fellow Ph.D. candidates, Priyatosh Jena, Rajat Kumar Keshari, and Virendra Prasad Maurya, for their valuable technical insights and unwavering support throughout this research journey. I am particularly thankful to my junior colleagues, Ankit, Warda, Manish, Aman, and Arya, for their contributions to maintaining a positive research environment within the laboratory. I would also like to thank IDD students Vinay and Rohan for their assistance throughout this journey.

I am sincerely thankful to all the Gurus (From school, B. Tech., M.Tech.) who have put their efforts into nurturing my life, and seniors and friends are constantly motivating me. I have always believed that expressing emotions for someone's contribution in words is hard. So, I wish them to be happy wherever they are.

I want to express my deepest gratitude to my family for their unwavering love and support throughout my academic journey. My parents, Late Nand Lal Barnawal and Smt. Madhuri Devi, my brother and sisters, and my wife Richa have consistently encouraged my pursuits and provided me with the unconditional support necessary to focus on my research. I am eternally grateful for their sacrifices and their belief in me.

(Prakash Ji Barnawal)

## List of Figures

<b>Figure</b>	<b>Caption</b>	<b>Page No.</b>
1.1	Renewable power additions made from different resources.	1
1.2	The annual addition of solar power worldwide.	2
1.3	A simple architecture of a solar-based microgrid.	2
1.4	A simple architecture of an isolated DC-DC converter-based solar microgrid.	3
1.5	PWM type voltage-fed isolated DC-DC Converters.	5
1.6	Transition of working voltage and current.	6
1.7	Circuit diagram of the conventional dual active bridge.	7
1.8	Types of the isolated DC-DC resonant converters.	8
1.9	Isolated DC-DC converter with an expandable impedance network at input.	11
1.10	Existing two-stage electrolytic capacitor-less system.	13
1.11	P-V and I-V curves.	14
1.12	Block diagram representation of the proposed two-stage system.	18
2.1	Circuit diagram of the dual half active bridge resonant converter.	21
2.2	Key operating waveform for the DHABRC.	22
2.3	Operation of the circuit in different operating intervals.	25
2.4	Circuit diagram of the proposed converter ADABRC.	27
2.5	Key operating waveform for the ADABRC.	27
2.6	FHA equivalent diagram of the DHABRC.	28
2.7	Variation of resonant parameters.	30
2.8	Equivalent circuit diagram for an intermediate switching transition state.	33
2.9	Plot for ZVS operating Region.	36
2.10	Variation of dead time.	37
2.11	The photograph of the experimental setup.	39
2.12	Steady-state simulation results of DHABRC.	42

2.13	Steady-state experimental results of DHABRC.	43
2.14	Absolute variations of theoretical data.	45
2.15	Measurement of film capacitor voltages.	46
2.16	Measurement of film capacitor voltages due to tolerance.	46
2.17	Steady-state simulation results of ADABRC.	49
2.18	Steady-state experimental results of ADABRC.	50
2.19	Efficiency curve for the DHABRC.	51
2.20	The loss distribution map for the proposed converter.	51
3.1	Circuit diagram of the solar panel integrated DHABRC.	54
3.2	Movement of solution particle of the PSO in search space.	55
3.3	Flowchart of the PSO algorithm.	56
3.4	Pulse generation using phase-shift angle obtained from the algorithm.	56
3.5	Simulation results for PSO.	61
3.6	Experimental results for PSO.	65
3.7	Social hierarchy of the grey wolves based on their dominance.	66
3.8	Movement of the grey wolves for hunting.	66
3.9	Experimental results under uniform irradiance conditions.	69
3.10	Experimental results for Partial Shading Conditions (PSCs).	72
4.1	Control structure of a grid tied three-phase voltage source inverter.	75
4.2	Block diagram representation of the Phase Locked Loop (PLL).	76
4.3	Conversion of the coordinate systems.	76
4.4	Transformation of axes from $\alpha$ - $\beta$ to $d$ - $q$ reference frame.	77
4.5	Block diagram representation of the SRF based PLL.	79
4.6	Block diagram representation of the control system for the PLL.	79
4.7	Bode plot of the PLL's transfer function.	80
4.8	Bode plot of the PLL ( $G_P(s)$ ) and $G_{PI}(s)$ with PI controller.	81
4.9	Bode plot of the PLL ( $G_P(s)$ ) and $G_{P2}(s)$ with K-factor controller.	82

4.10	Simulation results for the d-axis and q-axis voltages.	84
4.11	Circuit diagram representation of the VSI integrated with grid system.	84
4.12	General block diagram representation of the inner current control loop.	86
4.13	Block diagram representation of the current control.	87
4.14	Bode plot of the plant transfer function of the current control.	88
4.15	Block diagram presentation of the inner current control loop.	88
4.16	Bode plot of the current control loop with MOTC.	90
4.17	Step Response of the current control loop with MOTC.	91
4.18	General block diagram representation of the outer voltage control loop.	92
4.19	The block diagram representation of the voltage control plant.	93
4.20	The bode plot of the plant transfer function of the voltage control.	93
4.21	Block diagram presentation of the outer voltage control loop.	95
4.22	Bode plot of the voltage control loop with SOTC.	96
4.23	Shading Patterns chosen for simulation results.	99
4.24	Simulation results.	101
4.25	Photograph of the experimental setup	102
4.26	Experiment results for shaded conditions with resistive load	103
4.27	Simulation results for Grid tied conditions .	106
5.1	Diagram of Expandable input impedance-sourced isolated resonant converter.	109
5.2	Operating modes of proposed EIIS network	111
5.3	Operating waveform of proposed EIIS network.	112
5.4	Boundary condition between CCM and DCM.	115
5.5	Equivalent circuit diagram of the EIISIRC.	117
5.6	Waveforms of the EIISIRC in steady-state condition.	118
5.7	Effect of the quality factor.	123
5.8	Photograph of experimental Setup of EIISIRC.	127
5.9	Steady-state results of EIISIRC.	129

5.10	Soft-switching results.	130
5.11	Experimental results under UIC.	132
5.12	Experimental results for PSCs.	133
5.13	Experimental results showing dynamic irradiance.	134
5.14	Film capacitor voltages.	136
5.15	Expandable network (a) With fault (b) Without fault in C <sub>4</sub>	137

## List of Tables

<b>Table</b>	<b>Caption</b>	<b>Page No.</b>
2.1	Design parameters of DHABRC	40
2.2	Comparison table for the key parameters at steady-state condition	44
2.3	Design parameters of ADABRC	47
2.4	Comparison of proposed DHABRC with existing topologies	52
3.1	Design parameters of the solar PV integrated DHABRC and PSO	57
3.2	Parameters of the shading patterns for PSCs for simulation results	58
3.3	Parameters of the shading patterns for PSCs and experimental results	61
3.4	Parameters of selected PV curves for UIC and PSC testing using GWO	67
3.5	Comparison of proposed DHABRC with the existing converters	73
4.1	Clark and park transformation and their inverse transformation	77
4.2	Effect of the symmetricity coefficient on outer voltage control loop	97
4.3	Used design specifications of the topology	98
4.4	Parameters of the shading patterns chosen for simulation results	98
4.5	Parameters of the PV-curves for experimental results	104
4.6	Used design specifications of the ADABRC based two-stage topology	104
5.1	Comparative analysis	126
5.2	Design parameters of EIISIRC and PSO	128



## List of Acronyms

PV	Photovoltaic
MPPT	Maximum power point tracking
P&O	Perturb and observe
INC	Incremental Conductance
DHABRC	Dual half active bridge resonant converter
ADABRC	Asymmetrical dual half-active bridge resonant converters
UIC	Uniform irradiance conditions
PSC	Partial shading conditions
VSI	Voltage source inverter
EMI	Electromagnetic interference
EIISIRC	Expandable input impedance-sourced isolated resonant converter
DC	Direct current
EV	Electric vehicle
ZVS	Zero voltage switching
ZCS	Zero current switching
DAB	Dual active bridge
PSM	Phase-shift modulation
SRC	Series resonant converter
PRC	Parallel resonant converter
SPRC	Series-parallel resonant converter
qZSI	Quasi-Z-source Inverter
EC	Electrolytic capacitor

FC	Film capacitor
PSO	Particle swarm optimization
GWO	Grey wolf optimization
SRF	Synchronous reference frame
PLL	Phase locked loop
HFT	High-frequency transformer
FHA	Fundamental harmonics approximation
GP	Global peak
LP	Local peak
SP	Shading pattern
OLTF	Open loop transfer function
CLTF	Closed loop transfer function
GM	Gain margin
PM	Phase margin
SPWM	Sinusoidal pulse width modulation
ADC	Analog to digital conversion
MOTC	Modulus optimum tuning criterion
SOTC	Symmetrical optimum tuning criterion
THD	Total harmonics distortion
EIIS	Expandable input impedance source
CCM	Continuous conduction mode
DCM	Discontinuous conduction mode
GMP	Global maxima point
LMP	Local maxima point

## Symbols Used

$V_{in}, V_{PV}$	DC Input voltage
$I_{in}, I_{PV}$	Input current
$P_{PV}$	Input PV power
$V_o$	Output voltage
$I_o$	Output current
$P_o$	Output power
$C_1-C_4$	Film capacitors
$V_{C1}-V_{C4}$	Voltage across film capacitors
$L_r$	Resonant inductance
$C_r$	Resonant capacitor
$K$	Inductance ratio
$V_{Cr}$	Voltage across resonant capacitor
$L_m$	Parallel inductance
$S_1-S_4$	Active switches
$D_1-D_4$	Body diode of active switches
$n_t$	Turns ratio
$V_{AB}$	Primary bridge voltage
$i_r$	Primary bridge current
$V_{CD}$	Secondary bridge voltage
$i_s$	Secondary bridge current
$\phi$	Phase angle
$F_s$	Switching frequency of DC-DC converter
$I_{S1}-I_{S4}$	Switch current

$V_{GS1} - V_{GS4}$	Gating signals for DC-DC converter
$f_r$	Resonant frequency
$V_B$	Base voltage
$Z_B$	Base impedance
$\omega_B$	Base frequency
$M, \lambda$	Voltage gain
$F$	Normalized switching frequency
$Q$	Quality factor
$Z_{ac}$	AC impedance
$\alpha$	Lagging angle of primary bridge current
$\beta$	Leading angle of secondary bridge current
$C_{S1}-C_{S4}$	Parasitic capacitance of active switches
$T_{D\_P}$	Dead time primary switch
$T_{D\_S}$	Dead time secondary switch
$K$	Iteration number
$x_i$	Position vector
$v_i$	Velocity vector
$P_b$	Personal best
$G_b$	Global best
$w$	Inertia coefficient
$c_1 - c_2$	Cognitive and social weighting factor
$r_1 - r_2$	Random number
$\alpha_g$	Alpha wolves
$\beta_g$	Beta wolves

$\omega_g$	Omega waves
$\delta_g$	Delta waves
$X_p, X$	Position vector
$A, C_g$	Coefficient vector
$V_{DC}$	DC link voltage
$i_a, i_b, i_c$	Phase currents of grid
$E_a, E_b, E_c$	Grid line voltages
$v_a, v_b, v_c$	Grid phase voltages
$f_g$	Grid frequency
$L_f$ and $C_f$	Filtering capacitor
$TF$	Transfer function
$G_P$	Plant transfer function of PLL
$G_{P1}$	OLTF of PLL with PI controller
$G_{P2}$	OLTF of PLL with K-factor controller
$K_{pi}$	Proportional gain for inner current control loop
$K_{ii}$	Integral gain for inner current control loop
$T_i$	Integral time constant for inner current control loop
$K_{po}$	Proportional gain for outer voltage control loop
$K_{io}$	Integral gain for outer voltage control loop
$T_o$	Integral time constant for outer voltage control loop
$G_I$	OLTF of current control loop
$G_{I1}$	OLTF of current control loop with PI controller
$G_{CLI}$	CLTF of current control loop
$G_V$	OLTF of voltage control loop plant

$G_{V1}$	OLTF of voltage control loop with PI controller
$D$	Duty
$C_a - C_d$	Film Capacitor
$L_1, L_2, L_3$	Inductors
$V_{D0}, V_{D1}, V_{D2}$	Voltage across the diodes